Eduvest – Journal of Universal Studies
Volume 6 Number 2, February, 2026
p- ISSN 2775-3735- e-ISSN 2775-3727

In Silico Study: Metabolite Compounds of Zingiber Officinale Var. Rubrum as Potential E2F2 Inhibitor Agents in Breast Cancer Signaling Pathway

Khoirunnisa Purwamita Budiutami[1*], Aryo Tedjo[2], Fadilah[3], Surya Dwira[4], Ajeng M. Fajrin[5]
Universitas Indonesia
Emails: khoirunnisa.purwamita@ui.ac.id*, aryo.tedjo@ui.ac.id, fadilah@ui.ac.id, surya.dwira@ui.ac.id

ABSTRACT

Breast cancer ranks among the leading causes of death in women, linked to disruptions in signaling pathways regulating cell proliferation and survival, particularly E2F2 gene activity. E2F2 regulation falters when pRB is phosphorylated by Cyclin D–CDK4/6 or Cyclin E–CDK2 complexes, freeing E2F2 to activate cell cycle genes. This study, "In Silico Study: Metabolite Compounds of Zingiber officinale var. rubrum as Potential E2F2 Inhibitor Agents in Breast Cancer Signaling Pathway," assesses red ginger (Zingiber officinale var. rubrum) metabolites as CDK4/CDK6 inhibitors via molecular docking in silico. Target protein structures came from the Protein Data Bank; metabolites were chosen for reported anticancer effects and 3D-modeled. Docking used Molegro Virtual Docker to gauge ligand affinity and interactions at active sites. Results highlighted [12]-shogaol, (E,E)-α-farnesene, and 1-dehydro-[6]-gingerdione as CDK4 inhibitors; azafrin, [8]-shogaol, and [12]-shogaol for CDK6. These exhibit strong binding via hydrogen bonds and hydrophobic interactions at key residues. Red ginger metabolites show promise as CDK4/CDK6 inhibitors for breast cancer therapy, pending in vitro/in vivo validation.

KEYWORDS *molecular docking, red ginger, CDK4, CDK 6, bioinformatics*

INTRODUCTION

Breast cancer is one of the most common types of cancer found in women around the world. Based on the 2022 Global Cancer Statistics released by the World Health Organization (WHO), Indonesia had 408,661 new cancer cases and 242,988 cancer deaths. One type of cancer that is the focus of the problem in Indonesia is breast cancer (GLOBOCAN, 2022). In 2022, breast cancer ranked first as the cancer with the highest number of patients in Indonesia, at 66,271 cases or equivalent to 16.2%.¹ Based on molecular profile and receptor expression, breast cancer can be divided into several subtypes, each with different biological characteristics and responses to therapy. One of the most commonly found subtypes is luminal A, which is characterized by estrogen receptor (ER), progesterone receptor (PR) positive, and HER2 negative expression (Dubey et al., 2022).

Luminal A was chosen as a research subject because its molecular characteristics are closely related to hormone regulation, which makes it responsive to therapies that target hormone receptors (Diessner et al., 2016). This mechanism makes luminal A an ideal model for exploring the effects of hormone therapy and treatment alternatives in regulating cancer cell growth, particularly those that focus on signaling pathways that regulate cell proliferation (Piasecka et al., 2019; Sflomos et al., 2016; Telang, 2022; Yip & Papa, 2021). One of these is the signaling pathway involving E2F2, a major transcription factor in cell cycle regulation (Gao

et al., 2024). E2F2 dysregulation is often associated with cancer due to its role in promoting cell proliferation, making E2F2 an important therapeutic target (Kassab et al., 2023).

E2F2 plays a key role in the transition from the G1 phase to the S phase in the cell cycle by activating the transcription of target genes important for cell division (Chen et al., 2009; Elakkiya et al., 2025). E2F2 dysregulation can cause the activation of target genes to become uncontrollable (Firakania, 2015). E2F2 functions by binding to and regulating target genes involved in the cell cycle, but its regulation can be disrupted by the phosphorylation of pRB (retinoblastoma protein) by the Cyclin D–CDK4/6 or Cyclin E–CDK2 complexes, leading to the release of E2F2 and activation of genes that accelerate the cell cycle (Chen et al., 2009; Elakkiya et al., 2025; Kassab et al., 2023). Given its vital role in cell proliferation, the search for alternative anticancer agents that can inhibit E2F2 activity needs to be explored more deeply, especially those derived from natural materials.

Zingiber officinale var. rubrum, or better known as red ginger, has long been known for its biological activities, including anti-inflammatory (M. Zhang et al., 2016), antioxidant (Kumar et al., 2014), and antimicrobial (Nile & Park, 2015) effects. This is because it contains various bioactive compounds, such as phenolic and terpenoid compounds (Nanda, 2025). Examples of the main phenolic compounds that contribute to the biological activity of ginger are gingerol, shogaol, and paradol (Yusof, 2016; Nanda, 2025). Experimental results show that 6-shogaol, 6-gingerol, and oleoresin in ginger have very high antioxidant activity (Bischoff-Kont et al., 2022; Nanda, 2025). Antioxidants can suppress the excessive production of reactive oxygen species (ROS) in the body, thereby preventing oxidative stress. Excessively high ROS levels can damage cells and tissues because ROS can oxidize deoxyribonucleic acid (DNA), lipids, and proteins, initiating cancer (Kumar et al., 2015). Therefore, an approach is needed to test the active compounds of red ginger that can potentially be used as anticancer agents.

An in silico approach through molecular docking was selected to visualize the binding results of each red ginger metabolite compound at specific active sites on the target proteins CDK4 and CDK6. The results of this test may indicate red ginger metabolite compounds that are potential candidates, especially based on their ability as protein inhibitor agents in the E2F2 gene in the breast cancer cell cycle signaling pathway (Ali et al., 2025; Anandasadagopan et al., 2020; Hairunisa et al., 2023; Huang et al., 2021; Zhao et al., 2020).

Despite these promising properties, the specific molecular mechanisms underlying red ginger's anticancer effects—particularly its interaction with CDK4 and CDK6—remain poorly characterized. Previous studies have primarily focused on phenotypic observations of growth inhibition, with limited investigation into the molecular binding interactions at the protein level. Furthermore, no comprehensive comparative analysis has been conducted to identify which specific metabolites from red ginger exhibit the strongest affinity for CDK4/6 active sites.

To address these knowledge gaps, this study employs a molecular docking-based in silico approach to systematically evaluate the binding affinities and interaction patterns of 24 red ginger metabolite compounds with CDK4 and CDK6 proteins. This computational methodology enables rapid screening and rational identification of lead compounds prior to resource-intensive experimental validation. The novelty of this research lies in (1) the comprehensive screening of red ginger metabolites specifically against CDK4/6 targets in the context of E2F2-mediated breast cancer pathogenesis, (2) the detailed characterization of

molecular interaction patterns at atomic resolution, and (3) the comparative assessment with clinically relevant CDK inhibitors.

The objectives of this study are threefold: first, to predict the binding affinities of red ginger metabolite compounds toward CDK4 and CDK6 proteins through molecular docking simulations; second, to elucidate the molecular interaction patterns, including hydrogen bonding, hydrophobic contacts, and electrostatic interactions; and third, to identify the most promising metabolite candidates as potential CDK4/6 inhibitors based on computational scoring functions and interaction stability. The findings from this study are expected to provide a rational foundation for subsequent in vitro and in vivo experimental validation, ultimately contributing to the development of nature-derived therapeutic alternatives for breast cancer management.

METHOD

Molecular docking was performed to predict the binding interactions between the metabolite compounds contained in red ginger ethanol extract and the target protein in the E2F2 gene. The type of metabolite compounds contained in red ginger ethanol extract refers to research by Purwanto et al (2024). Furthermore, the CID code and structure of each metabolite compound from the study are accessed through the PubChem database page. Meanwhile, the crystal structure of the target protein was taken from the RSCB PDB database. The target proteins used are CDK4 (GDP ID: 9CSK) and CDK6 (GDP ID: 3NUX). The three-dimensional structure of CDK4 and CDK6 is obtained from the Protein Data Bank (PDB). This molecular docking is carried out using Molegro Virtual Docker software (MVD v7.0.0).

The PDB file of each protein is imported into the MVD and prepared using the Protein Preparation feature, which includes the removal of all water molecules and unnecessary co-crystalline ligands, as well as the correction of incomplete atoms or bonds. After that, cavity detection is carried out to identify cavities that correspond to the location of co-crystalline ligands at the ATP binding site, which is then selected as the main binding site. The cavity is named and stored, with the determination of the central coordinates and radius of the search space that includes the entire binding pocket and the surrounding key residues.

The structure of each of the previously downloaded red ginger metabolite compounds is then prepared by ligand minimization through the "Ligand Energy Inspector" feature to obtain a stable conformation. This feature includes 3D rebuild, addition of hydrogen atoms, charge determination, and identification and determination of rotating atoms to allow ligand flexibility during the docking process. Validation of the docking protocol is done first through re-docking native ligands (co-crystalline ligands) into the same cavity. Docking is set using the MolDock algorithm with the function of MolDock score and re-ranking score, number of runs 10–20, population size and max iterations following the default settings of the MVD. The re-docking results were then compared to the position of the initial crystallographic ligands, and the protocol was considered valid if the RMSD value between the docking position and the position of the native ligand was < 2.0 Å, for both CDK4 and CDK6.

After the protocol is validated, the main docking process is carried out by inserting all red ginger metabolites as ligands, docked to CDK4 and CDK6 receptors at their respective binding sites. The docking process is executed using the MolDock Optimizer algorithm with a number of runs of 20–30 per ligand to extend conformation exploration, while other parameters

such as population size, max iterations, and energy threshold are set based on the default recommendations. For each ligand and receptor, the MVD generates multiple poses with a MolDock score and a re-ranking score. The pose with the lowest energy is chosen as the best pose. Follow-up analysis was performed by visualizing the best poses in the MVD, observing the position of the ligands within the ATP-binding sac and their interaction patterns with key residues, including hydrogen bonds, hydrophobic interactions, and electrostatic interactions. Red ginger metabolite compounds that exhibit the lowest MolDock score and re-ranking score values and form stable and biologically relevant interactions at CDK4 and CDK6 active sites were identified as the most potential inhibitor candidates. The strength of the interaction is assessed based on energy parameters, such as MolDock Score, and Hbond, as well as Rerank Score as the main indicators.

RESULT AND DISCUSSION

Molecular docking simulation is a form of computational study in predicting interactions between molecules at the atomic scale, which involves modeling the three-dimensional structure between the target protein molecule and the ligand molecule(Anggraeni et al., 2025). The results of molecular docking show a prediction of the stability of the complex formed based on the calculation of the bond energy and its interaction (Anggraeni et al., 2025). Validation of the interaction between CDK4 (PDB ID: 9CSK) and the native ligand Atirmocilib (A1A_9001) in its crystal structure for the stage redocking is shown on Figure 1.

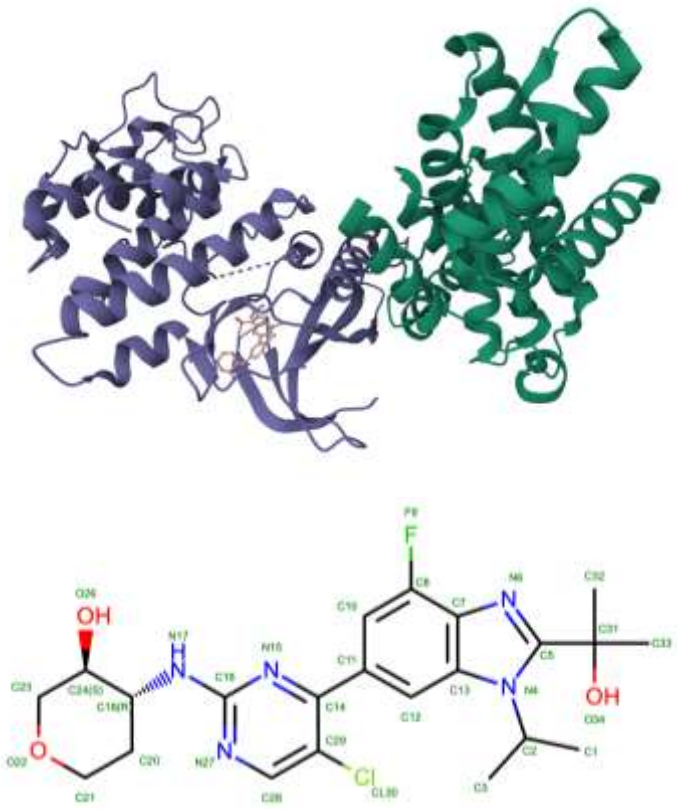

Figure 1. 3D structure of 9CSK protein (CDK4) and 2D structure of native ligand

The redocking stage showed ligands [00]A1A_9001 [B] had an RMSD result of less than 2Å, which was 1.02822Å with a rerank score of -116.774 kJ/mol so that it was declared valid (Table 1). Furthermore, molecular docking was carried out between CDK4 (PDB ID: 9CSK) and 24 metabolite compounds contained in Z. officinale var rubrum, including [12]-Shogaol, (E,E)-alpha-Farnesene, 1-Dehydro-[6]-gingerdione, [8]-Shogaol, [6]-Gingerdiol, [10]-Shogaol, [10]-Gingerol, [8]-Gingerdione, Methyl [6]-shogaol, 6-Gingerol, [6]-Shogaol, Gingerdione, 3,4-Dihydroxytamoxifen, 4-Hydroxytamoxifen, Phthalic acid, isobutyl octyl ester, [6]-Paradol, Azafrin, 5-(4-carboxy-3-methylbutyl)-5,6,8atrimethyl-3-oxo3,4,4a,5,6,7,8,8aoctahydronaphthalene-1- carboxylic acid, (+)-ar-Turmerone, Ethylcinnamate, Curcumene, Methylcinnamate, (+/-)-Camphor, Hecogenin.

Table 1. Rerank score and RMSD redocking result of A1A_9001 [B] compound as native ligand with CDK4 protein (PDB ID: 9CSK)

Ligand	Compound Name	MolDock Score (kJ/mol)	Rerank Score (kJ/mol)	RMSD (Â)	HBond (kJ/mol)
[00]A1A_9001 [B]	Atirmociclib	-137.128	-116.774	1.02822	-8.64262
[01]A1A_9001 [B]	Atirmocilib	-135.651	-112.539	1.04165	-7.88855

Table 2. Molecular docking results of *Z. officinale* var rubrum metabolite compounds with CDK4 protein(PDB ID: 9CSK)

Ligand	Compound Name	MolDock Score (kJ/mol)	Rerank Score (kJ/mol)	HBond (kJ/mol)
[00]A1A_9001 [B]	Atirmociclib (*native ligand*)	-136.853	-116.588	-8.5485
[04]5281225	Azafrin	-124.36	-108.477	-6.95603
[02]6442560	[8]-Shogaol	-127.844	-102.188	-2.25251
[01]9975813	[12]-Shogaol	-136.951	-99.722	0
[00]22321203	1-Dehydro-[6]-gingerdione	-119.61	-96.8938	-4.27437
[00]6442612	[10]-Shogaol	-118.432	-96.8495	-2.5
[04]10386463	3,4-Dihydroxytamoxifen	-123.012	-96.7134	-3.43077
[02]168115	[10]-Gingerol	-117.144	-94.006	-3.70856
[00]91721066	Methyl [6]-shogaol	-113.967	-92.6068	-0.71326
[00]442793	6-Gingerol	-119.332	-91.2687	-2.02683
[00]5275727	[6]-Gingerdiol	-117.609	-89.5232	-4.73306
[03]449459	4-Hydroxytamoxifen	-116.869	-89.1998	-3.06649
[03]14440537	[8]-Gingerdione	-111.225	-89.1331	-2.5
[00]11152	[6]-Shogaol	-114.379	-88.1459	-5.80925
[06]56776388	5-(4-carboxy-3-methylbutyl)-5,6,8atrimethyl-3-oxo3,4,4a,5,6,7,8,8aoctahydronaphthalene-1-carboxylic acid	-107.355	-85.2883	-4.46202
[01]94378	[6]-Paradol	-105.745	-84.6534	-1.23112
[05]162952	Gingerdione	-103.821	-84.6457	-2.88515
[03]6423815	Phthalic acid, isobutyl octyl ester	-101.204	-81.1354	0
[00]5281516	(E,E)-alpha-Farnesene	-97.2652	-79.3657	0
[00]160512	(+)-ar-Turmerone	-101.47	-76.8891	-3.16901
[00]92139	Curcumene	-90.7395	-68.9278	0
[01]637758	Ethylcinnamate	-79.0483	-68.8611	-2.37582
[04]637520	Methylcinnamate	-69.8397	-62.3214	0

[00]2537	(+/-)-Camphor	-53.8973	-50.2326	-2.5
[03]91453	Hecogenin	-77.2675	-50.1681	5.69578

Based on the rerank score, Atirmociclib as a native ligand has a rerank score of –116.588 kJ/mol with an H-bond score of –8.5485 kJ/mol (Table 2). Azafrin exhibits the highest affinity among the other 24 metabolites with a rerank score of –108.477 kJ/mol and a considerable contribution of hydrogen bonds (–6.95603 kJ/mol), so that the stability of the complex is closest to the native ligand of atirmociclib. [8]-Shogaol is next with a rerank score of –102.188 kJ/mol and HBond of –2.25251 kJ/mol, indicating that the affinity is still good but its hydrogen bonds are not as strong as Azafrin. Meanwhile, [12]-shogaol has a very low MolDock score but its rerank score is only –99.722 kJ/mol and shows no contribution to hydrogen bonding, so overall the complex is weaker than Azafrin, and is still below the native ligand. Thus, these three compounds have the potential to be alternative CDK4 inhibitors, but Atirmociclib remains the standard with the highest affinity and bond stability.

Visualization of the molecular docking results between CDK4 and the three best metabolite compounds, namely Azafrin, [8]-Shogaol, and [12]-Shogaol can be seen in Figure 2. In the interaction of CDK4 with native ligands, hydrogen bonds appear to be formed between the ligand's hydroxyl group with residues Asp158(B), Val 96(B), and His95(B) which function to maintain the orientation of the ligand molecule in the active pocket of the enzyme and increase the specificity of the bond. Steric interactions are seen between the aromatic ring and the nonpolar part of the ligand with residues of Lys 35(B), Phe93(B), Val96(B), and Ile12(B). This interaction supports the adjustment of the shape of the ligands within the active cavity of CDK4 thereby strengthening the van der Waals force and the overall stability of the complex. This combination of strong hydrogen bonds and extensive hydrophobic interactions explains Atirmociclib's very high binding affinity to CDK4.

The CDK4–Azafrin complex is stabilized primarily by electrostatic interactions with the negatively charged residues Glu74(A), Glu75(A), and Glu76(A), which attracts polar hydroxyl groups on Azafrin. This force plays an important role in maintaining the orientation of the ligand at the active site. In addition, there are steric (hydrophobic) interactions around the ligand cyclohexane ring that help balance the position and strengthen the stability of the complex. This suggests that Azafrinoccupies a stable position in the active pocket of CDK4 and is able to adapt well to the electrostatic environment of the enzyme. [8]-Shogaol, appears to dominate the steric bond line with residues of Glu74(A), Glu75(A), and Glu162(A). This bond indicates the presence of a repulsive force that indicates the match of the shape of the ligand around the glutamic acid group. In addition, there are a small number of electrostatic interactions that strengthen the orientation of molecules in the active cavity, but the intensity is not as strong as in the Azafrin ligand. In contrast, [12]-Shogaol exhibits only steric bonds involving nonpolar residues Ala157(B), Val20(B), and Val96(B), without strong electrostatic bond support. Although the three compounds have a fairly high match result and are close to the native ligand, the density and diversity of the bonds are not as strong and as directed as the native ligand, so their binding power to CDK4 is still below Atirmociclib.

Azafrin functions as a natural antioxidant that is cardioprotective by protecting heart cells from oxidative damage so that it has the potential to be used as an adjuvant for the prevention and therapy of ischemic heart disease (Yang et al., 2018; X. Zhang et al., 2019). In addition,

Azafrin is also one of the main metabolite compounds contained in saffron plants which has been shown to inhibit the growth of various cancer cell lines, such as colorectal cancer, breast, lung, prostate, cervix, as well as leukemia, glioblastoma, and rhabdomyosarcoma (Wang et al., 2022). 8-shogaol has anti-inflammatory and anticancer activity, in testing of gastric cancer cells of the AGS and NCI-N87 types, 8-shogaol has been shown to inhibit cell survival and at the same time trigger the mechanism of cell death (Kim & Lee, 2024).

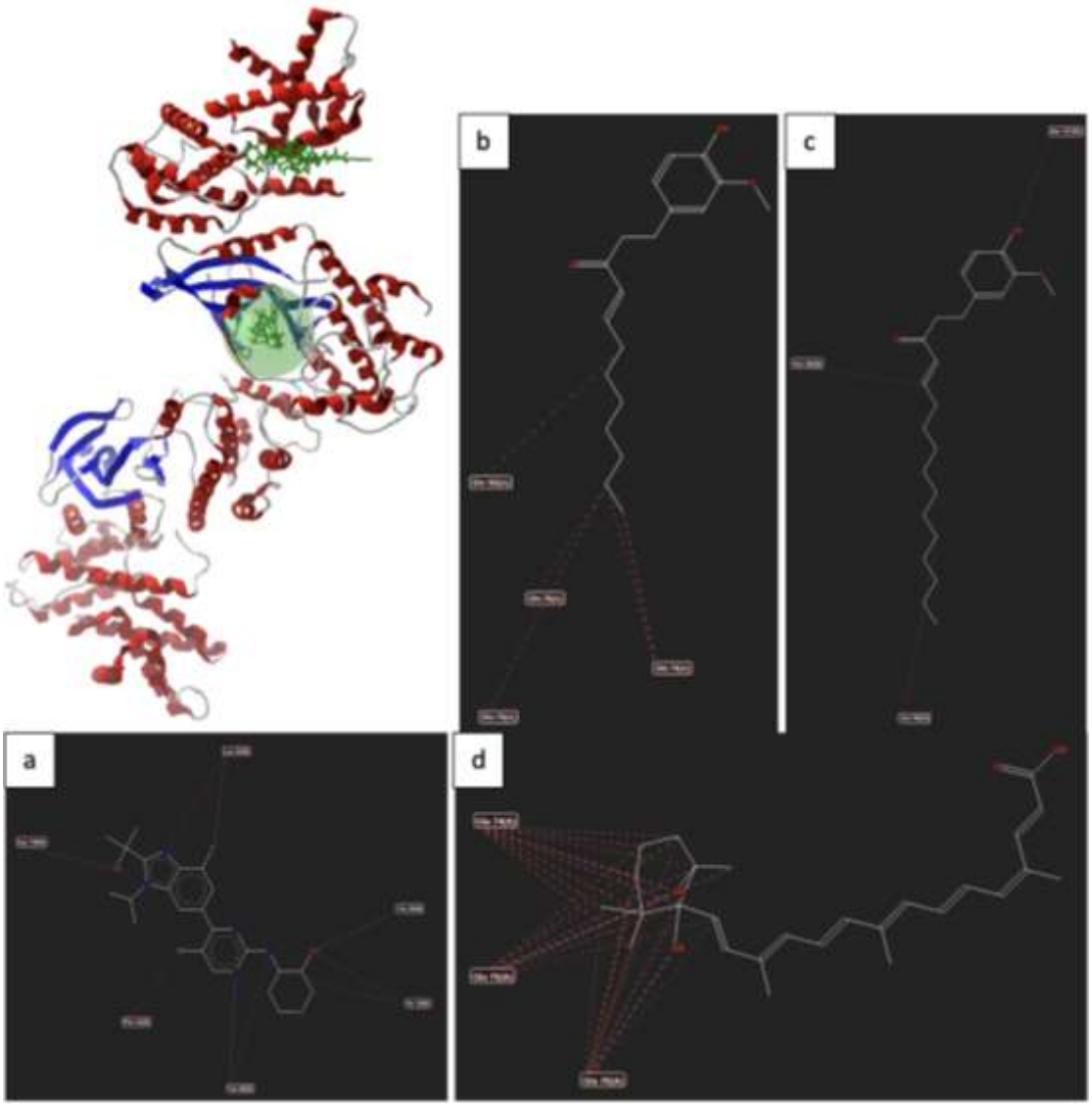

Figure 2. Molecular docking results visualization of protein CDK4 (PDB ID: 9CSK) with *Z. officinale* var rubrum metabolites; (a) complex with native ligand complex; (b) complex with [12]-Shogaol; (c) complex with [8]-Shogaol; (d) complex with Azafrin

CDK6 (PDB ID:3NUX), on the other hand, is seen for its compatibility with the crystal structure of the native ligands [03]3NV_900 [A] or 4-[5-chloro-3-(1-methylethyl) -1H-pyrazol-4-yl]-N-(5-piperazin-1-ylpyridin-2-yl) pyrimidin-2-amine through the redocking stage (Figure 2). The native ligand showed an RMSD value of 1.02822 Å (Table 3), which is still below the 2 Å threshold, accompanied by a rerank score of −52.6649 kJ/mol. The combination of these values indicates that the redocking results meet the validity criteria and correspond to

the structure of the reference crystal. The three best compounds with a rerank score close to native ligands (-105.433 kJ/mol), include [12]-Shogaol (-101.188 kJ/mol), (E,E)-alpha-Farnesene (-100.695 kJ/mol), and 1-Dehydro-[6]-gingerdione (-98.551 kJ/mol) (Table 4).

Table 3. Rerank score and RMSD redocking result of 3NV_900 [A] compound as native ligand with CDK6 protein (PDB ID: 3NUX)

Ligand	Nama Senyawa	MolDock Score (kJ/mol)	Rerank Score (kJ/mol)	RMSD (Â)	HBond (kJ/mol)
[03]3NV_900 [A]	4-[5-chloro-3-(1-methylethyl)-1H-pyrazol-4-yl]-N-(5-piperazin-1-ylpyridin-2-yl)pyrimidin-2-amine	-125.545	-52.6649	1.37758	-4.73212
[02]3NV_900 [A]	4-[5-chloro-3-(1-methylethyl)-1H-pyrazol-4-yl]-N-(5-piperazin-1-ylpyridin-2-yl)pyrimidin-2-amine	-127.142	-100.927	1.40895	-4.32258
[01]3NV_900 [A]	4-[5-chloro-3-(1-methylethyl)-1H-pyrazol-4-yl]-N-(5-piperazin-1-ylpyridin-2-yl)pyrimidin-2-amine	-138.905	-95.8115	1.80364	-4.56431
[00]3NV_900 [A]	4-[5-chloro-3-(1-methylethyl)-1H-pyrazol-4-yl]-N-(5-piperazin-1-ylpyridin-2-yl)pyrimidin-2-amine	-146.464	-106.573	1.80904	-3.99539

Table 4. Molecular docking results of *Z. officinale* var rubrum metabolite compounds with CDK6 protein (PDB ID: 3NUX)

Ligand	Compound Name	MolDock Score (kJ/mol)	Rerank Score (kJ/mol)	HBond (kJ/mol)
[03]3NV_900 [A]	4-[5-chloro-3-(1-methylethyl)-1H-pyrazol-4-yl]-N-(5-piperazin-1-ylpyridin-2-yl) pyrimidin-2-amine (*native ligand*)	-133.33	-105.433	-4.65121
[00]9975813	[12]-Shogaol	-128.525	-101.188	-1.18866
[08]5281225	(E,E)-alpha-Farnesene	-116.313	-100.695	-2.80946
[01]22321203	1-Dehydro-[6]-gingerdione	-113.579	-98.5515	-4.74377
[00]6442560	[8]-Shogaol	-123.949	-94.9147	-2.5
[00]5275727	[6]-Gingerdiol	-123.98	-92.9311	-3.7389
[00]6442612	[10]-Shogaol	-124.47	-92.8788	-2.4508
[05]168115	[10]-Gingerol	-113.647	-88.5821	-5.93927
[05]14440537	[8]-Gingerdione	-104.279	-88.4784	-0.19922
[00]91721066	Methyl [6]-shogaol	-108.802	-86.6909	-0.11728
[02]442793	6-Gingerol	-102.471	-85.1748	-1.22198
[02]11152	[6]-Shogaol	-103.206	-82.8133	-1.87143
[05]162952	Gingerdione	-103.513	-81.8743	-2.38637
[01]10386463	3,4-Dihydroxytamoxifen	-109.592	-81.4656	-5.02488
[02]449459	4-Hydroxytamoxifen	-110.843	-81.3932	0
[05]6423815	Phthalic acid, isobutyl octyl ester	-95.6888	-81.0673	-0.13389
[05]94378	[6]-Paradol	-99.2349	-79.7343	-2.43213

[02]5281516	Azafrin	-93.236	-75.4068	0
[06]56776388	5-(4-carboxy-3-methylbutyl)-5,6,8atrimethyl-3-oxo3,4,4a,5,6,7,8,8aoctahydronaphthalene-1-carboxylic acid	-100.892	-73.4757	-4.93678
[01]160512	(+)-ar-Turmerone	-81.5863	-66.9144	-0.43607
[01]637758	Ethylcinnamate	-74.115	-66.313	-1.39713
[09]92139	Curcumene	-74.9909	-63.7587	0
[01]637520	Methylcinnamate	-66.0093	-59.7116	-1.62827
[02]2537	(+/-)-Camphor	-43.8642	-40.9002	-2.5
[06]91453	Hecogenin	4.73431	265.974	0

The interaction between CDK6 and native ligands [03]3NV_900 [A] involving hydrogen bonds is formed between the ligand's nitrogen group with the residues of Lys43, Val101, and Glu99, which plays a role in maintaining the stability of the ligand's orientation within the active sac of the enzyme (Figure 3). Meanwhile, steric interactions occur in residues of His100, Val101, and Ala162,z aromatic rings and nonpolar parts of the ligand adapt to the hydrophobic environment via van der Waals force. The combination of these two types of bonds suggests that ligands [03]3NV_900 [A] have a stable binding position and are spatially matched to the active site of CDK6, supporting their role as natural inhibitors of the protein.

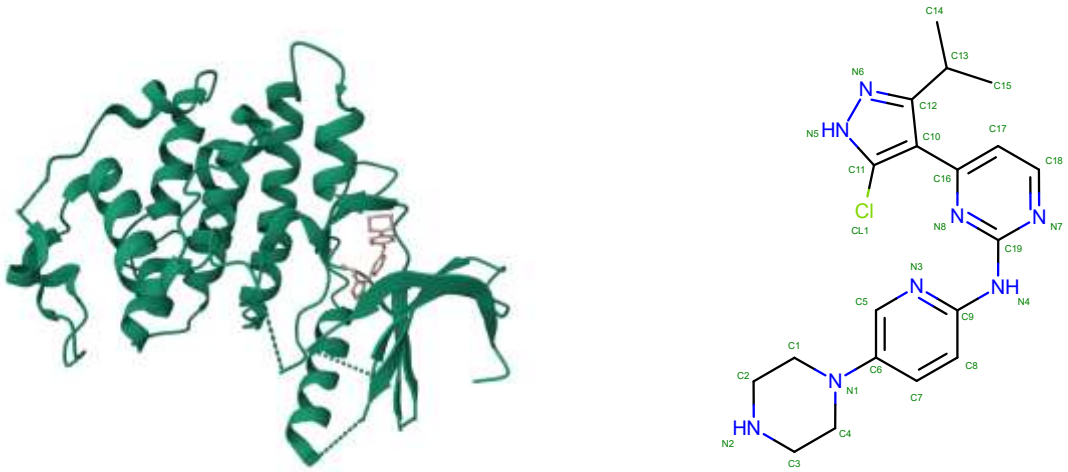

Figure 3. 3D structure of CDK6 protein (PDB ID: 3NUX) and 2D structure of native ligand

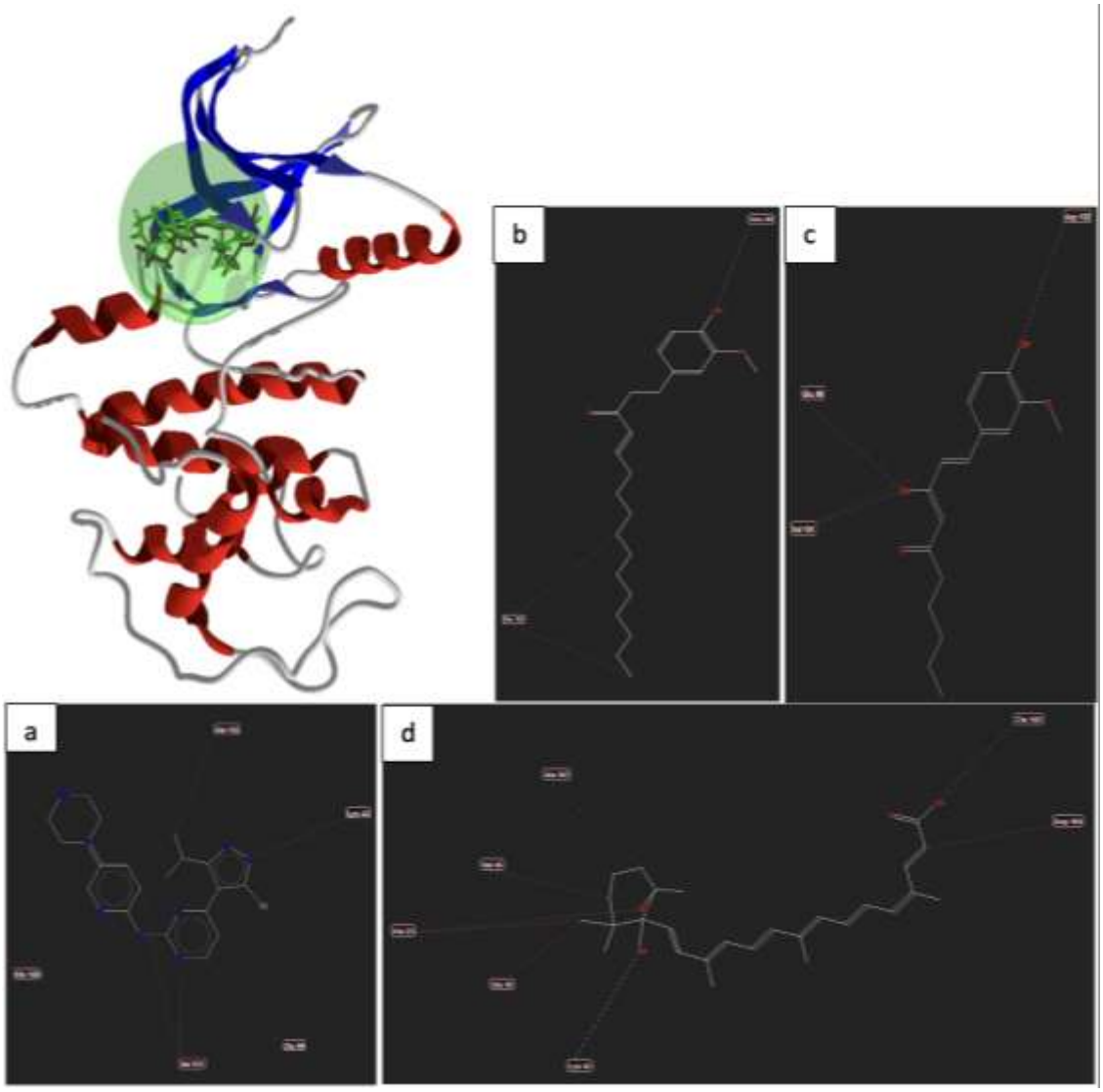

Figure 4. Molecular docking results visualization of protein CDK6 (PDB ID: 3NUX) with *Z. officinale* var rubrum metabolites; (a) complex with native ligand; (b) complex with [12]-Shogaol; (c) complex with 1-Dehydro-[6]-gingerdione; (d)kompleks dengan (E,E)-alpha-Farnesene

The results of the visualization of molecular docking between CDK6 and the three best metabolite compounds can be seen in figure 4. [12]-Shogaol forms a hydrogen bond with Glu99 and aliphatic tail-long steric contact with Ile19, so that despite the contribution of small hydrogen bond values (−1,189 kJ/mol), the fit of the active pocket shape makes its energy closest to the native ligand. α-Farnesene is predominantly steric bonds with Ala23, Gly25, Val45, Ala167, Asp104, accompanied by hydrogen bonds Thr107 and electrostatic bonds Lys43, a stable combination, but still below [12]-Shogaol. 1-Dehydro-[6]-gingerdione forms the strongest hydrogen bond net (−4,743 kJ/mol) in Glu99, Val101, Asp102 and Val101 steric bonds, but the overall pose is less than optimal and therefore the rerank is higher. Thus, [12]-Shogaol is the best candidate in total with the lowest energy among metabolites and the presence of steric bond support.

CONCLUSION

Zingiber officinale var extract. rubrum shows potential as an anticancer agent through the mechanism of inhibition of CDK4 and CDK6 proteins, which play an important role in the regulation of cell cycle transition from the G1 to S phase. The results of molecular docking and energy map analysis identified several active metabolites such as [12]-Shogaol, (E,E)-α-Farnesene, and 1-Dehydro-[6]-gingerdione as potential inhibitors for CDK4 proteins, while Azafrin, [8]-Shogaol, and [12]-Shogaol as potential inhibitors for CDK6 proteins. The compound has a fairly strong binding affinity at the active sites of CDK 4 and CDK 6 proteins. Follow-up studies in vivo are needed to confirm the effectiveness of the metabolites of Z. officinale var. rubrum in suppressing E2F2 expression as well as to evaluate its potential synergies with conventional CDK inhibitors.

REFERENCES

Ali, M. L., Noushin, F., Sadia, Q. A., Metu, A. F., Meem, J. N., Chowdhury, M. T., Rasel, M. H., Suma, K. J., Alim, M. A., & Jalil, M. A. (2025). Spices and culinary herbs for the prevention and treatment of breast cancer: A comprehensive review with mechanistic insights. *Cancer Pathogenesis and Therapy*, 3(3), 197–214.

Anandasadagopan, S. K., Sivaprakasam, P., Pathmanapan, S., Pandurangan, A. K., & Alagumuthu, T. (2020). Targeting the key signaling pathways in breast cancer treatment using natural agents. In *Plant-derived bioactives: Chemistry and mode of action* (pp. 137–183). Springer.

Bischoff-Kont, I., Primke, T., Niebergall, L. S., Zech, T., & Fürst, R. (2022). Ginger constituent 6-shogaol inhibits inflammation- and angiogenesis-related cell functions in primary human endothelial cells. *Frontiers in Pharmacology*, 13, 844767. https://doi.org/10.3389/fphar.2022.844767

Diessner, J., Wischnewsky, M., Blettner, M., Häusler, S., Janni, W., Kreienberg, R., Stein, R., Stüber, T., Schwentner, L., Bartmann, C., & Wöckel, A. (2016). Do patients with luminal A breast cancer profit from adjuvant systemic therapy? A retrospective multicenter study. *PLOS ONE*, 11(12), e0168730. https://doi.org/10.1371/journal.pone.0168730

Dubey, S. K., Bhatt, T., Agrawal, M., Saha, R. N., Saraf, S., Saraf, S., & Alexander, A. (2022). Application of chitosan modified nanocarriers in breast cancer. *International Journal of Biological Macromolecules*, 194, 521–538. https://doi.org/10.1016/j.ijbiomac.2021.11.095

Elakkiya, M. R., Krishnasreya, M., Tharani, S., Arun, M., Vijayalakshmi, L., Lim, J., Ghfar, A. A., & Chithradevi, B. (2025). Targeting CDK4/6 in cancer: Molecular docking and cytotoxic evaluation of *Thottea siliquosa* root extract. *Biomedicines*, 13(7), 1658. https://doi.org/10.3390/biomedicines13071658

Gao, Y., Qiao, X., Liu, Z., & Zhang, W. (2024). The role of E2F2 in cancer progression and its value as a therapeutic target. *Frontiers in Immunology*, 15, 1397303. https://doi.org/10.3389/fimmu.2024.1397303

Hairunisa, I., Bakar, M. F. A., Da'i, M., Bakar, F. I. A., & Syamsul, E. S. (2023). Cytotoxic activity, anti-migration, and *in silico* study of black ginger (*Kaempferia parviflora*) extract against breast cancer cells. *Cancers*, 15(10), 2785. https://doi.org/10.3390/cancers15102785

Huang, P., Zhou, P., Liang, Y., Wu, J., Wu, G., Xu, R., Dai, Y., Guo, Q., Lu, H., & Chen, Q. (2021). Exploring the molecular targets and mechanisms of [10]-gingerol for treating triple-negative breast cancer using bioinformatics approaches, molecular docking, and

in vivo experiments. *Translational Cancer Research*, 10(11), 4680–4693.

Kassab, A., Gupta, I., & Al Moustafa, A. E. (2023). Role of E2F transcription factor in oral cancer: Recent insight and advancements. *Seminars in Cancer Biology*, 92, 28–41. https://doi.org/10.1016/j.semcancer.2023.03.004

Kim, T. W., & Lee, H. G. (2024). Anti-inflammatory 8-shogaol mediates apoptosis by inducing oxidative stress and sensitizes radioresistance in gastric cancer. *International Journal of Molecular Sciences*, 26(1), 173. https://doi.org/10.3390/ijms26010173

Kumar, A., Hussain, S., Yadav, I. S., Gissmann, L., Natarajan, K., Das, B. C., & Bharadwaj, M. (2015). Identification of human papillomavirus-16 E6 variation in cervical cancer and their impact on T and B cell epitopes. *Journal of Virological Methods*, 218, 51–58. https://doi.org/10.1016/j.jviromet.2015.03.008

Nile, S. H., & Park, S. W. (2015). Chromatographic analysis, antioxidant, anti-inflammatory, and xanthine oxidase inhibitory activities of ginger extracts and its reference compounds. *Industrial Crops and Products*, 70, 238–244. https://doi.org/10.1016/j.indcrop.2015.03.033

Piasecka, D., Braun, M., Kitowska, K., Mieczkowski, K., Kordek, R., Sadej, R., & Romańska, H. (2019). FGFs/FGFRs-dependent signalling in regulation of steroid hormone receptors—Implications for therapy of luminal breast cancer. *Journal of Experimental & Clinical Cancer Research*, 38(1), 230.

Sflomos, G., Dormoy, V., Metsalu, T., Jeitziner, R., Battista, L., Scabia, V., Raffoul, W., Delaloye, J.-F., Treboux, A., & Fiche, M. (2016). A preclinical model for ERα-positive breast cancer points to the epithelial microenvironment as determinant of luminal phenotype and hormone response. *Cancer Cell*, 29(3), 407–422.

Telang, N. T. (2022). The divergent effects of ovarian steroid hormones in the MCF-7 model for luminal A breast cancer: Mechanistic leads for therapy. *International Journal of Molecular Sciences*, 23(9), 4800. https://doi.org/10.3390/ijms23094800

Wang, C.-Z., Ma, Q., Kim, S., Wang, D. H., Shoyama, Y., & Yuan, C.-S. (2022). Effects of saffron and its active constituent crocin on cancer management: A narrative review. *Longhua Chinese Medicine*, 5, 35. https://doi.org/10.21037/lcm-21-72

Yang, S., Chou, G., & Li, Q. (2018). Cardioprotective role of azafrin against myocardial injury in rats via activation of the Nrf2–ARE pathway. *Phytomedicine*, 47, 12–22. https://doi.org/10.1016/j.phymed.2018.04.042

Yip, H. Y. K., & Papa, A. (2021). Signaling pathways in cancer: Therapeutic targets, combinatorial treatments, and new developments. *Cells*, 10(3), 659. https://doi.org/10.3390/cells10030659

Zhang, M., Viennois, E., Prasad, M., Zhang, Y., Wang, L., Zhang, Z., Han, M. K., Xiao, B., Xu, C., Srinivasan, S., & Merlin, D. (2016). Edible ginger-derived nanoparticles: A novel therapeutic approach for the prevention and treatment of inflammatory bowel disease and colitis-associated cancer. *Biomaterials*, 101, 321–340. https://doi.org/10.1016/j.biomaterials.2016.06.018

Zhang, X., Li, C., Wang, L., Fei, Y., Qin, W., Zhang, X., Li, C., Wang, L., Fei, Y., & Qin, W. (2019). Analysis of *Centranthera grandiflora* Benth transcriptome explores genes of catalpol, acteoside, and azafrin biosynthesis. *International Journal of Molecular Sciences*, 20(23), 6034. https://doi.org/10.3390/ijms20236034

Zhao, L., Rupji, M., Choudhary, I., Osan, R., Kapoor, S., Zhang, H.-J., Yang, C., & Aneja, R. (2020). Efficacy-based ginger fingerprinting reveals potential antiproliferative analytes for triple-negative breast cancer. *Scientific Reports*, 10(1), 19182. https://doi.org/10.1038/s41598-020-76220-3